

## Observation of an Unconventional Metal-Insulator Transition in Overdoped $\text{CuO}_2$ Compounds

F. Venturini,<sup>1</sup> M. Opel,<sup>1</sup> T. P. Devereaux,<sup>2</sup> J. K. Freericks,<sup>3</sup> I. Tüttő,<sup>4</sup> B. Revaz,<sup>5</sup> E. Walker,<sup>5</sup> H. Berger,<sup>6</sup>  
L. Forró,<sup>6</sup> and R. Hackl<sup>1</sup>

<sup>1</sup>Walther Meissner Institute, Bavarian Academy of Sciences, 85748 Garching, Germany

<sup>2</sup>Department of Physics, University of Waterloo, Waterloo, Ontario, Canada N2L 3G1

<sup>3</sup>Department of Physics, Georgetown University, Washington, D.C. 20057

<sup>4</sup>RISPO, Hungarian Academy of Sciences, P.O.Box 49, 1525 Budapest, Hungary

<sup>5</sup>DPMC, University of Geneva, 1121 Genève, Switzerland

<sup>6</sup>EPFL, Ecublens, 1025 Lausanne, Switzerland

(Received 26 April 2002; published 19 August 2002)

The electron dynamics in the normal state of  $\text{Bi}_2\text{Sr}_2\text{CaCu}_2\text{O}_{8+\delta}$  is studied by inelastic light scattering over a wide range of doping. A strong anisotropy of the electron relaxation is found which cannot be explained by single-particle properties alone. The results strongly indicate the presence of an unconventional quantum-critical metal-insulator transition where “hot” (antinode) quasiparticles become insulating while “cold” (node) quasiparticles remain metallic. A phenomenology is developed which allows a quantitative understanding of the Raman results and provides a scenario which links single- and many-particle properties.

DOI: 10.1103/PhysRevLett.89.107003

PACS numbers: 74.72.-h, 71.30.+h, 78.30.-j

The normal state of copper-oxygen compounds is characterized by several crossover lines separating regions of the phase diagram with different physical properties [1]. The line usually identified with the opening of a pseudogap at  $T^*$  has been observed in many experiments which probe both single-particle properties such as specific heat, angle-resolved photoemission (ARPES), and many-particle properties such as NMR and transport [2,3]. An additional crossover at higher temperatures and doping has been determined from anomalies in NMR at  $T_0$  [4]. Moreover, another temperature scale  $T_{MI}$  associated with a metal-insulator transition has been found in transport [5]. Although several scenarios have been proposed [6–12], there is no consensus of whether and how  $T^*$ ,  $T_0$ , and  $T_{MI}$  are related. It would be extremely useful if a description of electron dynamics could be able to connect the results from various experiments to a common origin.

From the point of view of critical phenomena it is not uncommon that single-particle properties may show substantially different behavior from many-particle properties [13]. In the vicinity of a quantum phase transition (QPT) single-particle properties, e.g., density of states at the Fermi level, may be uncritical, while two-particle properties such as the conductivity may deviate from Fermi-liquid behavior. For studying a putative QPT in planar anisotropic systems like the copper-oxygen compounds a method is desirable which not only probes many-particle properties but also has resolution in  $\mathbf{k}$  space. Raman scattering of light by electrons can indeed meet these requirements in that the dynamical response can be measured for different regions in the Brillouin zone due to the possibility to independently adjust the polarizations of incoming and outgoing photons. Thus, the  $B_{1g}$  and  $B_{2g}$  electronic Raman spectra can probe either “hot” (antinode) or “cold” (no-

dal) electrons with momenta along the principal axes and the diagonals of the  $\text{CuO}_2$  plane, respectively.

In this paper we present results from Raman scattering experiments in  $\text{Bi}_2\text{Sr}_2\text{CaCu}_2\text{O}_{8+\delta}$  (Bi2212) over a wide range of effective doping  $0.09 < p < 0.24$ . We show that the transport of hot electrons vanishes already at very high doping levels while the cold ones still display metallic behavior. We propose a phenomenology which can describe the results quantitatively and outline how the various regimes in the phase diagram could be connected.

The experiments have been performed on a set of single crystals with different doping levels. We started from an extremely homogeneous overdoped Bi2212 crystal grown by the traveling solvent floating zone method with a  $T_c$  of 78 K and a transition width of only 0.2 K. From this specimen several pieces were cut and annealed at 620 K in oxygen partial pressures of 300 and 1350 bar to obtain transition temperatures of 62 and 56 K, respectively.

Raw data of the Raman response  $\chi''_{\mu}(\omega, T, p)$  (with the symmetry index  $\mu = B_{1g}, B_{2g}$ ) for various temperatures are plotted in Fig. 1. Superimposed on the broad electronic continua are narrow bands originating from Raman-active lattice vibrations. The overall continua for  $B_{2g}$  symmetry (bottom row) are relatively doping independent and show a low-energy response,  $\omega < 200 \text{ cm}^{-1}$ , which decreases with increasing  $T$ . In contrast, for  $B_{1g}$  symmetry (top row) the continua show nontrivial dependence on doping and  $T$ : the low-energy response decreases with increasing  $T$  in a similar way as in  $B_{2g}$  symmetry for the strongly overdoped sample [Fig. 1(e)], becomes essentially temperature independent for  $0.16 \leq p \leq 0.20$  [Fig. 1(c), [14]], and increases with increasing  $T$  for samples below optimum doping [Fig. 1(a)]. The different doping dependences for the two symmetries become strikingly evident if

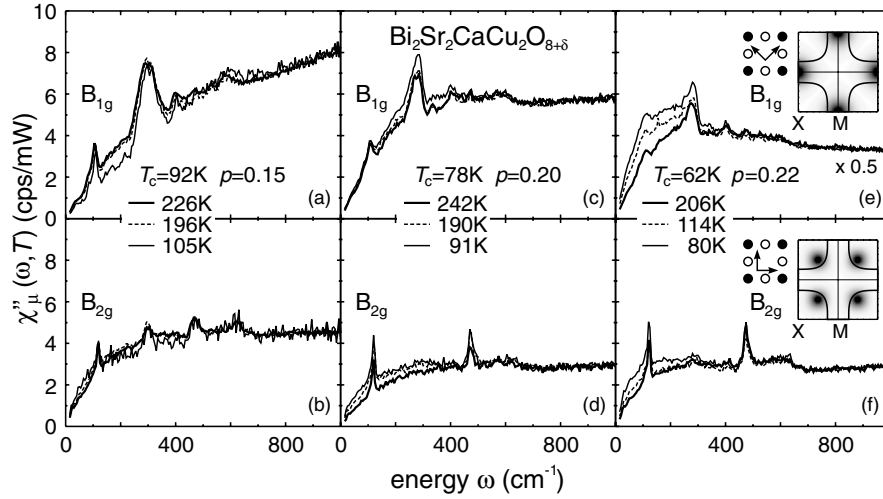


FIG. 1. Raman response  $\chi''_{\mu}(\omega, T, p)$  ( $\mu = B_{1g}, B_{2g}$ ) of  $\text{Bi}_2\text{Sr}_2\text{CaCu}_2\text{O}_{8+\delta}$ . The effective doping levels  $p$  are derived from the empirical relation  $p = 0.16 \mp 0.11\sqrt{1 - T_c/T_c^{\text{max}}}$  [2]. The spectra in the top row are measured for  $B_{1g}$  symmetry [polarizations of the incoming and outgoing light perpendicular and at  $45^\circ$  to the copper (solid symbols) oxygen (open symbols) bonds]. For this configuration, the sensitivity is highest around the M points and vanishes along the diagonals of the Brillouin zone. The Fermi surface is indicated as a bold line [see inset of (e)]. For  $B_{2g}$  symmetry (bottom row), the centers of the quadrants are projected out while the principal axes become invisible [inset of (f)].

the spectra are plotted at a fixed temperature  $T \approx 180$  K as a function of carrier concentration  $p$  as shown in Fig. 2. For  $B_{2g}$  symmetry [Fig. 2(b)] the doping dependence is very weak. For  $B_{1g}$  symmetry [Fig. 2(a)] the response is suppressed strongly with decreasing doping in an energy range of about  $2000 \text{ cm}^{-1}$  indicating the existence of a gap of this magnitude for the hot electrons.

In order to link the results to momentum-dependent electron dynamics we analyze the electronic Raman response in the dc limit,  $\omega \rightarrow 0$ . For nonresonant scattering we obtain [15]

$$\chi''_{\mu}(\omega \rightarrow 0) = \omega N_F \left\langle \gamma_{\mu}^2(\mathbf{k}) \int d\xi \left( -\frac{\partial f^0}{\partial \xi} \right) \frac{Z_{\mathbf{k}}^2(\xi, T)}{2\Sigma''_{\mathbf{k}}(\xi, T)} \right\rangle. \quad (1)$$

Here  $N_F$  is the density of electronic levels at the Fermi energy  $E_F$  and  $\gamma_{\mu}(\mathbf{k})$  is the Raman scattering amplitude, dependent upon incident (scattered) photon polarizations  $\hat{e}_{I(S)}$  corresponding to different symmetries  $\mu = B_{1g}, B_{2g}$ .  $\Sigma''_{\mathbf{k}}$  is the imaginary part of the single-particle self-energy related to the electron lifetime as  $\hbar/2\Sigma''_{\mathbf{k}}(\omega, T) = \tau_{\mathbf{k}}(\omega, T)$ ,  $Z_{\mathbf{k}}(\omega, T)$  is the quasiparticle residue,  $f^0$  is the Fermi distribution function, and  $\langle \dots \rangle$  denotes an average over the Fermi surface.

Using Eq. (1) we can define the Raman relaxation rate via the slope of the spectra in the dc limit,  $\Gamma_{\mu}(T) \equiv N_F \langle \gamma_{\mu}^2(\mathbf{k}) \rangle [\partial \chi''_{\mu}(\omega \rightarrow 0, T) / \partial \omega]^{-1}$ . For an isotropic conventional metal one obtains  $\Gamma_{\mu}(T) = \hbar/\tau(T)$ . In a correlated or a disordered metal, however, a finite energy might be necessary to move an electron from one site to another one. Thus, in spite of a nonvanishing density of states at the

Fermi level as observed in an ARPES experiment, for instance, no current can be transported and  $\Gamma_{\mu}(T) \gg \hbar/\tau(T)$ .

$\Gamma_{\mu}(T)$  can be explicitly extracted from the Raman spectra by employing a memory or relaxation function approach [14,16]. In Fig. 3(a) Raman relaxation rates at a fixed temperature  $T = 200$  K obtained in this and previous studies [14] are compiled. The magnitude of  $\Gamma_{B_{1g}}$  decreases by approximately 70% for  $0.09 \leq p \leq 0.22$ , while  $\Gamma_{B_{2g}}$  is almost constant up to  $p \approx 0.20$  and changes by only 30% in

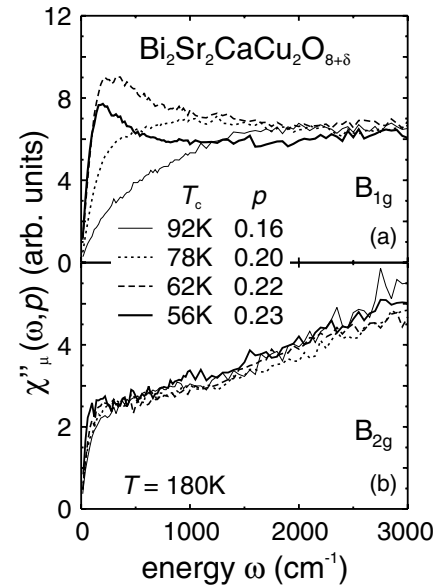


FIG. 2. Raman spectra  $\chi''_{\mu}(\omega, p)$  as a function of doping on an extended energy scale. For clarity the contributions from lattice vibrations have been subtracted out.

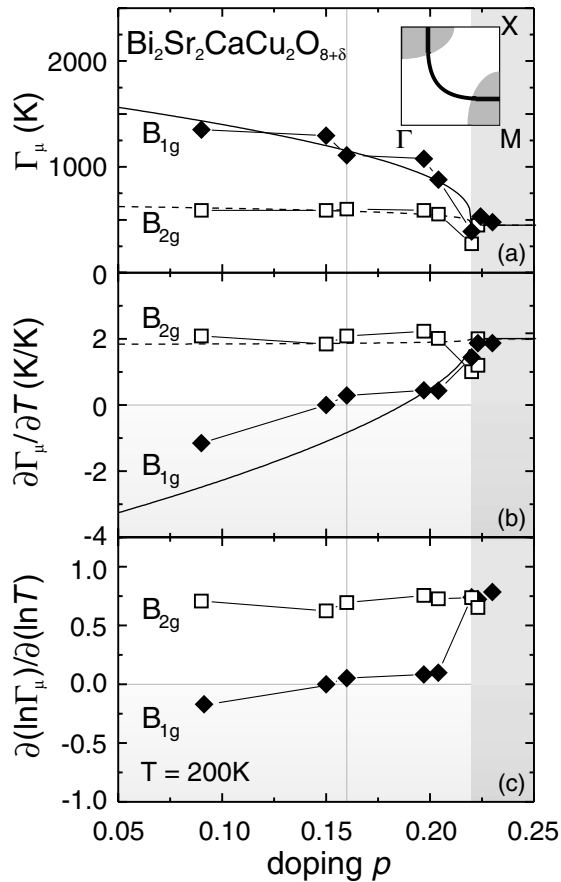


FIG. 3. (a) Raman relaxation rates  $\Gamma_\mu(p)$  as a function of doping  $p$ . The smooth lines are fits to the data employing Eq. (2) with a  $\mathbf{k}$ -dependent gap with the maxima close to the M points (inset). The metallic part above  $p_c = 0.22$  is shaded. The vertical line corresponds to optimum doping. (b)  $\partial\Gamma_\mu(T)/\partial T$  as a function of doping. The smooth lines are theoretical predictions. (c) Logarithmic derivatives of the Raman relaxation rates indicating power-law behavior in the temperature dependence.

the narrow range  $0.20 < p < 0.22$ . The abrupt crossover for  $0.20 < p < 0.22$  is remarkable: the Raman relaxation rates rapidly decrease, and the anisotropy vanishes. We emphasize that the changes for  $0.20 < p < 0.22$  are observed for a set of samples prepared from a single homogeneous piece and that the results agree well with those from earlier experiments; hence the observed features are robust. The variations of the relaxation rates with temperature  $\partial\Gamma_\mu(T)/\partial T$  as a function of doping are shown in Fig. 3(b).  $\partial\Gamma_{B_{2g}}(T)/\partial T$  (nodal electrons) deviates only a little from 2 in the entire doping range. The logarithmic derivative  $\partial[\ln\Gamma_{B_{2g}}(T)]/\partial(\ln T)$  [Fig. 3(c)] demonstrates that  $\Gamma_{B_{2g}}(T)$  varies essentially linearly with temperature. The two properties combined yield  $\Gamma_{B_{2g}}(T) \approx 2k_B T$ . In contrast, both  $\partial\Gamma_{B_{1g}}(T)/\partial T$  and  $\partial(\ln\Gamma_{B_{1g}}(T))/\partial(\ln T)$  (antinodal electrons) are strongly temperature dependent, increase continuously with  $p$ , and change sign close to

optimum doping. For  $p \geq 0.22$  any kind of anisotropy disappears.

It is both the apparent symmetry dependence of the Raman relaxation rates,  $\Gamma_{B_{2g}} < \Gamma_{B_{1g}}$  [Fig. 3(a)] and their characteristic increase towards lower temperature,  $\partial\Gamma_{B_{1g}}(T)/\partial T < 0$  for  $p \leq 0.16$  [Fig. 3(b)] which indicate that there is not only gaplike behavior but also a strong anisotropy of the gap with the maxima located around the M points [see Fig. 3(a)]. Thus the hot electrons show a crossover from metallic to insulating behavior near optimum doping, while the cold ones are metallic for all doping levels at the temperatures examined. This is what we call an anisotropic or generalized metal-insulator transition (MIT) as opposed to a conventional Mott transition [17] since the charge excitations become gapped only on parts of the Fermi surface, and the overall dc transport is still metallic.

The momentum dependence of the gap is reminiscent of both the superconducting gap and the pseudogap [2,3] being compatible with  $|d_{x^2-y^2}|$  symmetry. In spite of a similar  $\mathbf{k}$  dependence, however, an incipient superconducting instability (preformed pairs) can be safely excluded because of the high temperature (200 K) and doping level ( $p > 0.19$ ) of our experiment. The same holds for the pseudogap. Its onset temperature  $T^*$  actually merges with  $T_c$  already for  $0.16 < p < 0.19$  [2,3]. The scenario we have in mind here is that of an anisotropic charge gap which develops near the hot spots to minimize strong interactions between electrons [18]. Therefore, we examine the effect of an anisotropic normal-state gap on the Raman response.

An exact treatment of nonresonant electronic Raman scattering in systems displaying a quantum-critical MIT in the limit of infinite dimensions has been formulated for Hamiltonians displaying both Fermi-liquid and non-Fermi-liquid ground states [19]. However, the nature of a MIT in physical dimensions, the development of an anisotropic gap, and their effect on the Raman response is still an open issue. Rather than speculating on what drives the QPT we consider here a phenomenological treatment for a system near a QPT possessing a doping-dependent anisotropic gap in the charge channel  $\Delta_C(p)$ . The result can be directly derived from Eq. (1) using the following approximations: (1) we assume that the wave function renormalization factor is constant,  $Z_{\mathbf{k}}(\omega, T) \equiv Z$ , and nonzero only for  $\Delta_C \leq |\hbar\omega| \leq E_b$ , e.g., for frequencies located in either part of the band with a total width  $E_b$  separated symmetrically with respect to the chemical potential by  $\pm\Delta_C/2$  [20], (2) we take the imaginary part of the self-energy to be momentum, energy, and doping independent,  $\Sigma_{\mathbf{k}}''(\omega, T) = \Sigma''(T)$ , (3) we assume a simple momentum dependence of the gap which is compatible with the observed  $\mathbf{k}$  dependence,  $\Delta_C(\mathbf{k}, p) = \Delta_C(\varphi, p) \equiv \Delta_C^0(p) \cos^2(2\varphi)$  with  $\varphi$  the azimuthal angle on a cylindrical Fermi surface, and (4) the doping dependence of the gap is postulated to be proportional to  $(1 - p/p_c)^\zeta$  for

$p \leq p_c$ . We obtain for  $\Delta_C(p)$ ,  $k_B T \ll E_b$

$$\frac{\Gamma_\mu(p, T)}{2\Sigma''(T)} = \begin{cases} \frac{1}{2}[1 + \exp(\frac{\Delta_C^\mu(p)}{2k_B T})] & (\text{insulator}), \\ 1 & (\text{metal}). \end{cases} \quad (2)$$

$\Delta_C^\mu(p)$  is a symmetry-specific effective gap resulting from the Fermi-surface integration using  $\gamma_{B_{1g}}(\varphi) \sim \cos(2\varphi)$ , and  $\gamma_{B_{2g}}(\varphi) \sim \sin(2\varphi)$ .

In Fig. 3 along with the data, we plot theoretical curves calculated from Eq. (2) using  $\Sigma''(T) = k_B T$  (being qualitatively compatible with ARPES results in a wide range of doping [21]),  $\Delta_C^0/k_B = 1100$  K, and  $\zeta = 0.25$ . For the  $B_{2g}$  symmetry which, according to our previous studies, reflects dc and optical transport properties [14], the influence of the gap is weak, and the temperature dependence comes essentially from  $\Sigma''(T)$ . The general trend of the  $B_{1g}$  rates, in particular, the sign change, is well reproduced by the phenomenology. It cannot be derived from single-particle properties which, to our present knowledge, depend only negligibly on doping in the range studied [22]. Because of the selection rules or, equivalently, the weighted Fermi-surface average [Eq. (1)] the MIT is particularly well resolved in the Raman experiment and can be observed clearly up to its onset at  $0.21 \leq p \leq 0.22$ .

This strongly suggests that an underlying quantum-critical point for this material lies at a doping of  $p_c \approx 0.22$  which is higher than  $p_c^* \approx 0.19$  as derived from, e.g., transport and specific heat [2,3,5]. Nevertheless, it appears that the two phenomena are directly linked. The differences in the critical doping in transport and Raman can readily be traced back to the selection rules and directly reflect the unconventional anisotropic nature of the transition. Since  $p_c \approx 0.22$  is also inferred from the  $T_0$  line [1], Raman scattering probably captures the first onset of non-Fermi-liquid behavior in this compound similarly as NMR and can trace it back to a correlation-induced localization of carriers in restricted areas of the Fermi surface. On the other hand, the pseudogap at  $T^*$  does not fit straightforwardly into this scenario. It either marks a pairing or charge-ordering instability or is connected to  $T_0$  in a more complicated way through fluctuation effects [10].

The existence of a QPT seems to be a general feature of the cuprates although the critical doping depends on the material class as demonstrated for low  $T_c$  compounds [5]. Here we have shown that the QPT can be described phenomenologically in terms of a generalized MIT with a strongly anisotropic gap. In this framework the Raman data can be explained quantitatively and reconciled with the single-particle results from ARPES. Why  $p_c$  is smaller in systems with lower  $T_c$ 's remains an important question.

Many clarifying discussions with B. S. Chandrasekhar, D. Einzel, and A. Virosztek are gratefully acknowledged. F. V. is indebted to the Gottlieb Daimler-Karl Benz Foundation for financial support. T. P. D. acknowledges support from NSERC and PREA. The work is part of the DFG project under Grant No. HA2071/2-1. J. K. F. acknowledges support from NSF under Grant No. DMR-9973225.

- 
- [1] M. Gutmann, E.S. Božin, and S.J.L. Billinge, cond-mat/0009141.
  - [2] J. L. Tallon and J. W. Loram, *Physica (Amsterdam)* **349C**, 53 (2001).
  - [3] T. Timusk and B. W. Statt, *Rep. Prog. Phys.* **62**, 61 (1999).
  - [4] H. Alloul, T. Ohno, and P. Mendels, *Phys. Rev. Lett.* **63**, 1700 (1989).
  - [5] Y. Ando *et al.*, *Phys. Rev. Lett.* **75**, 4662 (1995); **77**, 2065 (1996); **79**, 2595 (1997); *Phys. Rev. B* **56**, R8530 (1997); G. S. Boebinger *et al.*, *Phys. Rev. Lett.* **77**, 5417 (1996); P. Fournier *et al.*, *ibid.* **81**, 4720 (1998); S. Ono *et al.*, *ibid.* **85**, 638 (2000).
  - [6] J. Zaanen and O. Gunnarsson, *Phys. Rev. B* **40**, 7391 (1989).
  - [7] A. Sokol and D. Pines, *Phys. Rev. Lett.* **71**, 2813 (1993).
  - [8] V. J. Emery and S. A. Kivelson, *Nature (London)* **374**, 434 (1995).
  - [9] S. C. Zhang, *Science* **275**, 1089 (1997).
  - [10] S. Andergassen *et al.*, *Phys. Rev. Lett.* **87**, 056401 (2001).
  - [11] C. M. Varma, *Phys. Rev. B* **61**, R3804 (2000).
  - [12] S. Chakravarty *et al.*, *Phys. Rev. B* **63**, 094503 (2001).
  - [13] S. Sachdev, *Science* **288**, 475 (2000).
  - [14] M. Opel *et al.*, *Phys. Rev. B* **61**, 9752 (2000).
  - [15] T. P. Devereaux and A. P. Kampf, *Phys. Rev. B* **59**, 6411 (1999).
  - [16] J. G. Naeini *et al.*, *Can. J. Phys.* **78**, 483 (2000).
  - [17] N. Mott, *Conduction in Non-Crystalline Materials* (Clarendon Press, Oxford, 1987).
  - [18] N. Furukawa *et al.*, *Phys. Rev. Lett.* **81**, 3195 (1998); J. González *et al.*, *Phys. Rev. Lett.* **84**, 4930 (2000).
  - [19] J. K. Freericks and T. P. Devereaux, *Phys. Rev. B* **64**, 125110 (2001); J. K. Freericks, T. P. Devereaux, and R. Bulla, *Phys. Rev. B* **64**, 233114 (2001).
  - [20] As shown for a marginal Fermi liquid, for instance,  $Z = 0$  does not necessarily imply that one cannot observe a Fermi surface. The approximation is therefore not in conflict with ARPES. In general, the gap  $\Delta_C$  should be considered an activation energy for moving a particle rather than a single-particle gap.
  - [21] M. R. Norman, M. Randeria, H. Ding, and J. C. Campuzano, *Phys. Rev. B* **57**, R11093 (1998); T. Valla, A. V. Fedorov, P. D. Johnson, Q. Li, G. D. Gu, and N. Koshizuka, *Phys. Rev. Lett.* **85**, 828 (2000).
  - [22] A. A. Kordyuk *et al.*, *Phys. Rev. B* **66**, 014502 (2002).